TWELFTH EUROPEAN ROTORCRAFT FORUM

Paper No. 59

INVESTIGATION OF GROUND AND AIR RESONANCE USING A COMBINATION OF MULTIBLADE COORDINATES AND FLOQUET THEORY

Jochen Ewald
Institute of Flight Mechanics
Technical University of Braunschweig

September 22 - 25, 1986

Garmisch-Partenkirchen
Federal Republic of Germany

Deutsche Gesellschaft für Luft- und Raumfahrt e. V. (DFVLR)
Godesberger Allee 70, D-5300 Bonn 2, F.R.G.

INVESTIGATION OF GROUND AND AIR RESONANCE USING A COMBINATION OF MULTIBLADE COORDINATES AND FLOQUET THEORY

J. Ewald
Institut für Flugmechanik
Technische Universität Braunschweig

1. Abstract

The description of the dynamic behavior of helicopters often leads to differential equations with periodically-varying coefficients. The solution of these differential equations can be obtained by different mathematical methods. An efficient procedure results from the combination of multiblade coordinates and Floquet theory. Using this method, investigations of ground and air resonance are carried out.

By plotting the eigensolutions and eigenvector functions it is shown that the transformation using multiblade coordinates do not eliminate the periodicity of the coefficients, and this not only by reason of different dynamic behavior of rotorblades but also by special frequencies contained in the system matrices. This paper includes the consideration of systems having such characteristics.

2. Notation

a_o, a_1, b_1, b_o	- flap-coefficients
a	- distance flap hinge to hub
b	- distance lag hinge to one point of the blade
$\underline{b}_k(t)$	- eigenfunction of the system with periodically varying parameters
$\underline{b}_k(0)$	- eigenvector of the Monodromy matrix
c_ζ, c_β	- stiffness parameters of rotor blade
d_ζ, d_β	- damping parameters of rotor blade
e_o, e_1, f_1, f_o	- lag-coefficients
e	- distance flap hinge to lag hinge
m	- mass of fuselage
m_b	- mass of one blade
R	- radius of rotor disc
$\underline{\underline{R}}$	- matrix of the corresponding system with constant parameters
T	- period of the periodic coefficients
t	- time
x, y	- degrees of freedom of the fuselage
$\underline{\hat{x}}_k$	- eigenvector of a system with constant parameters
β, ζ	- degrees of freedom of the rotor blade
ϑ_o, ϑ_c, ϑ_s	- collective and cyclic pitch
$\Delta(...)$	- perturbation value
δ_k	- real part of λ_k
ω_k	- imaginary part of λ_k
ω_k^*	- frequency obtained by Floquet-theory
λ_k	- eigenvalue of the corresponding system matrix with constant coefficients
Λ_k	- eigenvalue of Monodromy matrix
Ω	- rotor speed
$\underline{\underline{\Phi}}(t)$	- transition matrix
$\underline{\underline{\Phi}}(t=T)$	- Monodromy matrix

3. Introduction

Due to the coupling of the movements of the rotating blades and those of the fuselage, the mathematical description of the dynamic helicopter reaction leads to a differential equation system with periodically-varying coefficients. In order to solve this equation system, a variety of mathematical methods can be resorted to, especially the Fourier coordinate transformation which is also named multiblade coordinate transformation, and the Floquet theory.

With the help of the multiblade coordinates, the differential equation system with periodically varying coefficients can be explained by a corresponding differential equation system with constant coefficients which always exist according to the law of reduciability of Liapunow. By calculating the eigenvalues, the stability and natural frequency data can be determined directly and are easy to interpret. However, it is necessary that the system characteristics are subject to certain conditions so that the periodic coefficients in the equations really do disappear after insertion of the multiblade coordinates and the following indispensable analytical transformation of the equation.

When applying the Floquet theory, the system characteristics are not subject to any condition except that of the coefficients to be periodic. On the one hand, the stability of the system can also be discussed easily on the basis of the results; on the other hand the frequencies of the system cannot be determined directly. One should not make use of the term 'natural frequency' here, as - strictly seen - this is important for systems with constant coefficients only. This will be taken into consideration in the following.

However, when combining the multiblade coordinate transformation and the Floquet theory, the advantages of each can be combined and thus results can be obtained which are easy to interpret. Additionally, it is possible to consider blade to blade dissimilarities in the dynamic behavior. In the following, this method is presented exemplarily on the basis of investigations of ground and air resonance. The emphasis here is only to allow a comparison with other investigations of the ground and air resonance. New physical points of view are only of minor importance.

Fig. 1 shows the basic mechanical substitute model. Besides the two translatory degrees of freedom in x and y direction, the fuselage additionally has two rotationary motions: body pitch and body roll. Every single blade can perform lag as well as flap motion. A detailed deduction of the equations of motion can be found in /1/.

In order to carry out a very simplified investigation of air resonance, only the landing gear stiffness and dampers are put to zero. Of course, it is only the hover state that can be regarded.

4. Method of Solution

The following multiblade coordinates are introduced in the equations of motion for the lag and flap motion of the individual blades of a four-blade rotor:

$$\beta_k = a_o(t) - a_1(t)\,\cos\psi_k - b_1(t)\,\sin\psi_k + b_o(t)\,(-1)^{k-1}$$

$$\zeta_k = e_o(t) + e_1(t)\,\cos\psi_k + f_1(t)\,\sin\psi_k + f_o(t)\,(-1)^{k-1}$$

$$\beta_k(t) = a_o + \Delta a_o(t) - (a_1 + \Delta a_1(t))\,\cos\psi_k(t) - (b_1 + \Delta b_1(t))\,\sin\psi_k(t) - \Delta b_o(t)\,(-1)^{k-1}$$

$$\zeta_k(t) = e_o + \Delta e_o(t) + (e_1 + \Delta e_1(t))\,\cos\psi_k(t) + (f_1 + \Delta f_1(t))\,\sin\psi_k(t) + \Delta f_o(t)\,(-1)^{k-1} \qquad (1)$$

In order to eliminate the periodically-varying coefficients in the blade equations, the individual equations would additionally have to be multiplied with the multiblade coordinate coefficients and subsequently be added. The procedure is described in detail for example by J. Dugundij and J.H. Wendell /2/ as well as K.H. Hohenemser and S.K. Yin /3/.

However, these analytical transformations are not carried out here. This way, the differential equation system furtheron has periodically-varying coefficients. Using the Floquet theory, the eigenvalues Λ of the transition matrix $\underline{\Phi}^*$ which are also named characteristic multipliers, are determined. These are sufficient for stability statements. However, the frequencies which are typical for the system, are also interesting in most of the cases. In a system with constant coefficients, it is the natural frequencies that, like the modal dampings, result from the eigenvalue analysis. In a system with periodically-varying coefficients, there is a large spectrum of modulated rotor-harmonic frequencies instead of one eigenfrequency.

According to Liapunow's law of reduciability, there is a corresponding system with constant coefficients for every differential equation system with periodically-varying parameters. The eigenvalues of this system can be determined from the characteristic multipliers. The real part results in

$$\delta_k = \frac{1}{T} \ln |\Lambda_k|$$

and the imaginary part in

$$\omega_k = n\Omega \pm \frac{1}{T} \arg\Lambda_k . \qquad (2)$$

Due to the periodicity of the tan-function, the imaginary part is mathematically undetermined by an integral multiple of the rotor cycle frequency. However, this imaginary part is identical with an eigenfrequency of the corresponding system with constant coefficients and consequently can be clearly determined. In /1/, two methods are described regarding the development of the eigenfrequency curves as functions of the rotor cycle frequency. Starting from small rotor angle velocities or taking advantage of 'resonance conditions', the integral multiple of the rotor cycle frequency is determined and this way the eigenfrequency itself.

While the solution of the differential equation system with constant coefficients is brought about as a product of the constant eigenvector and the e-function

$$\underline{x}_k(t) = \hat{\underline{x}}_k \cdot e^{\lambda_k t} \qquad (3)$$

the solution of the system with periodically-varying coefficients is represented as

$$\underline{x}_k(t) = \underline{b}_k(t) \cdot e^{\lambda_k t} \qquad (4)$$

with $\underline{b}_k(t)$ as a time-dependent vector, which for this reason is called eigenvector function in the following. Essentially, the equation (4) only serves as a comparison of a system with periodically-varying coefficients on the one hand and a system with constant coefficients on the other. In a system with periodically-varying coefficients, it is an advantage to calculate the temporal solution according to the following relationship

$$\underline{x}_k(t) = \underline{\Phi}(t) \cdot \underline{b}_k(0) \qquad (5)$$

with $\underline{\Phi}(t)$ representing the transition matrix at any moment of time t and $\underline{b}_k(0)$ the k-th eigenvector of the specific transition matrix $\underline{\Phi}^*$ (t=T) at the end of one rotor revolution, which is also named 'Monodromy Matrix'. Consequently, the eigenvector function $\underline{b}_k(t)$ can be determined by multiplication of $e^{-\lambda_k t}$:

$$\underline{b}_k(t) = \underline{\Phi}(t) \cdot \underline{b}_k(0) \cdot e^{-\lambda_k t} \qquad (6)$$

For plotting purposes, the conjugate complex parts are taken into consideration as well, resulting in purely real functions. However, this calculation is rather extensive as two program runs are needed. As a first step, the monodromy matrix $\underline{\underline{\Phi}}^*$ is calculated as well as its eigenvalues and eigenvectors. In the second run the temporal solution $\underline{x}_k(t)$ or the eigenvector function $b_k(t)$ is worked out. Storage of the transition matrix $\underline{\underline{\Phi}}(t)$ according to any time step Δt would be an alternative, this, however, would require an extensive storage.

With the identical blade characteristics, the multiblade coordinates mostly describe the corresponding system with constant coefficients. The belonging system matrix is marked with $\underline{\underline{R}}$. The relationship between this system matrix $\underline{\underline{R}}$ and the transition matrix $\underline{\underline{\Phi}}^*(T)$ is described by the following equation:

$$\underline{\underline{\Phi}}^* = e^{\underline{\underline{R}}T} \qquad (7)$$

On the one hand, the eigenvalue calculation of the corresponding system with constant coefficients (equation 2) results from this equation, on the other hand it becomes evident that the transition matrix $\underline{\underline{\Phi}}^*$ and the constant system matrix $\underline{\underline{R}}$ have equal eigenvectors. Consequently, with the multiblade coordinates describing the system with constant coefficients, the accompanying modes of vibration are also known in this case. Thus, the extensive calculation of the eigenvector functions can be abandoned.

In order to control this, the time solution of the k-th natural value was calculated on the basis of the Floquet theory according to equation 5 and represented in fig. 2. The amplitude courses of the individual degrees of freedom are plotted against the time t. At last, multiplication with $e^{-(\delta + i\omega^*)_k t}$ leads to the eigenvector function. As it has been supposed, the diagram reveals the time-independent eigenvector $b_k(0)$. Consequently, the frequency share ω^* from the Floquet theory corresponds to an eigenfrequency.

Fig. 3 shows a diagram of the time solution and the eigenvector function calculated according to it for another eigenvalue. In the eigenvector function, the amplitudes are not constant, but oscillate with the same frequency which is just an integral multiple of the rotor cycle frequency. In this case the eigenfrequency ω derives from the part ω^* of the Floquet calculation +/- the integral multiple of the rotor cycle frequency. Here, the factor n can be read off directly. The algebraic sign can either be determined from the course of the eigenvector function or, as the eigenfrequency itself, from the course of the time solution. After multiplying the time solution with $e^{-\lambda t}$ where the real eigenfrequency being inserted, the time-independent eigenvector $\underline{b}_k(0)$ of the transition matrix is naturally brought about again.

5. Results

As a first application of the mathematical process described above, the ground resonance of a light helicopter with a hingeless rotor was investigated. The chosen data of the fuselage and the rotor and also the results (fig. 4) are already laid down in /1/ and serve to have a closer look at the problem in the following: The above diagram (fig. 4) shows the real parts of the eigenvalues, calculated for the constant system, and plotted against the rotor cycle frequency. The figure below reveals the belonging imaginary parts of the eigenvalues, i.e. the eigenfrequencies of the system with constant coefficients. The frequency curves are carried out according to the method described in /1/ from the results of the Floquet calculation. They are represented by the dotted line as an example. The course of all the frequency curves, especially the determination of the integral multiple of the rotor cycle frequency, could be confirmed by the calculation and graphic representation of the eigenvector functions.

On the ordinates the eigenfrequencies and damping values of the uncoupled motions are marked which are calculated from the data. Curves 5 and 6 show the collective mode of the flap frequency, curve 7 the corresponding progressing mode, and curve 4 the regressing mode. The belonging damping values, the real parts of the characteristic exponents (as the eigenvalues of the corresponding system with constant coefficients are also named) increase extremely with the rotor rotational speed, as the aerodynamic damping has a large influence on the flap motion. The curves 2 and 3 in the diagram below belong to the identical collecitve modes of the lag motion. Curve 12 shows the corresponding regressing mode of the lag frequency. Here, the course of the regressing mode is typical for a hingeless soft-in-plane rotor. The progressing mode of the lag frequency and the respective frequencies of the fuselage are changing into one another successively; this behavior is not only being carried out in the respective frequencies, but also in the belonging modal dampings, as shown in the diagram of the real parts. An example is the harsh transition of curve 9 from the roll damping to the damping of the x and y motion in the real part diagram and the corresponding transition of the frequency curve 9 from ω_Φ to $\omega_{x,y}$ in the diagram below.

The transition from a principally rolling motion into a strongly-coupled motion of the fuselage, that means a motion in x and y direction as well as roll motion, is also indicated by plotting the eigenvector function (fig. 5) for the respective range of the rotor rotational speed.

Fig. 6 shows the change of the mode of vibration corresponding to curve 10 of the eigenvalue diagram: With increasing rotational speed, the body-pitch motion changes into an almost pure progressing lag mode, resulting at last in a body roll mode. This transition is also shown in the flap motion which is coupled with the motion of the fuselage.

The eigenvalue diagrams show that a possible instability would firstly occur with $\Omega \approx 50$ rad/s as then the regressing lag frequency is identical with the lowest natural frequency of the fuselage, the eigenfrequency of the pitch motion. The belonging damping curve in the real part diagram, however, still shows sufficient damping for the critical rotational speed range. In the area of the resonance frequency, that means at a rotor angular velocity of about 50 rad/s, it is not only the frequencies that are identical, but the corresponding modes of vibration as well (fig. 7). When the rotor rotational speed is increased, the amplitude of the lag motion in the regressing lag mode becomes smaller, the part of the body pitch motion changes into a body roll motion, because the next possible instability can occur when regressing lag frequency and body roll frequency correspond to each other.

The vibration forms of the progressing and regressing flap frequency are merely coupled with the other degrees of freedom.

The modes of vibration of the collective frequencies in flap and lag motion are not at all coupled with the fuselage degrees of freedom. Besides the summation mode a_o and e_o, the multiblade coordinate approach also includes the difference mode b_o and f_o as new degrees of freedom corresponding to a four-blade rotor. As for instance J. Dugandij and J.H. Wendell have shown in /2/, the analytical transformation of the differential equation system with periodically-varying parameters into a system with constant coefficients leads to a partial decoupling of the equation of motions. Moreover, summation form a_o, e_o and difference form b_o and f_o are described by uncoupled equations that are identical. The consequence is that when calculating the eigenvalues, a double eigenvalue exists for the flap as well as the lag motion respectively. For such a double value, the corresponding modes of vibration are not determined by two eigenvectors, but by an eigenplane. Consequently, the mathematical process, calculating the eigenvectors determines two orthogonal vectors in this plane as eigenvectors. In doing so, either the modes of vibration shown in fig. 8 can come into existence which - as shown analytically in /2/ - include a decoupling of difference and summation mode or coupled modes come into being, as exemplarily shown in fig. 9.

Influence of collective and cyclic pitch angles

Regarding the calculations mentioned so far control inputs were not taken into consideration, i.e. collective and cyclic blade pitch angles had been put to zero. In the following, the influences of the control inputs are considered as well. To do this, the stationary values of the multiblade coordinates

$$a_{oo},\ a_{10},\ b_{10},\ e_{oo},\ e_{10},\ f_{10}$$

are determined in a trim calculation as a function of the blade pitch angles. With a growing collective blade pitch, the flap conus angle a_o is increased as well as the lag angle e_o due to the higher drag. When the course of the eigenvalues of the corresponding system with constant coefficients is recorded in the complex plane as a function of the collective blade pitch angle ϑ_o as a parameter (fig. 10), the destabilizing influence of the flap conus angle becomes evident, which has often been described in literature /4, 5/. Essentially, the regressing lag mode is influenced which is to a large extent coupled with the body pitch mode. At a collective blade pitch angle of $\vartheta_o \approx 9^o$, the regressing lag mode at last becomes unstable. At the same time, the stability of the body pitch mode increases with a growing collective blade pitch angle. When the distance between the rotor angular velocity and the resonance frequency $\Omega \approx 50$ rad/s becomes larger, this influence decreases. Here, a decisive term is the Coriolis force

$$F_{Co} = 2\,\Omega\,(e + b)\,\dot{\beta}\,\sin\beta, \qquad (8)$$

which excites the lag motion.

It is also noticable that the progressive flap damping decreases with increasing collective pitch ϑ_o. This can only be due to the air drag as can be shown in the calculation without aerodynamic damping (fig. 11) with flap conus angle a_o and lag angle e_o being varied directly, avoiding a trim calculation. Here, the eigenvalues of the flap motion are only insignificantly dependent on the conus angle although the damping of the flap motion now has extremely smaller values. Even at a flap conus angle of $a_o = 1{,}4^o$ compared with an angle of $a_o = 3{,}5^o$ belonging to the calculation including aerodynamic damping, the regressing lag mode becomes unsteady.

Due to the Coriolis force as well as the air drag, the increasing blade pitch angle ϑ_o or, respectively, the flap conus angle which consequently also increases, effects a coupling of flap and lag motion. Besides all the other modes of vibration, this becomes also apparent in the coupling of the collective and progressive modes of the flap and lag motion, which occurred totally separat with the zero blade pitch angle (fig. 12). However, there is no change of the modes of vibration besides this intensified coupling of the flap and lag degrees of freedom. This changes when the cyclic control inputs increase.

Fig. 13a shows the body roll mode with a collective pitch angle of $\vartheta_o = 8^o$ and, correspondingly, a cyclic pitch angle of $\vartheta_s = 8^o$. For reasons of comparison, the body roll mode with $\vartheta_s = 0^o$ can be seen in fig. 13b. In fig. 13a with $\vartheta_s \neq 0^o$, the frequencies vary in the different coordinates. Moreover, the vibrations of the individual degrees of freedom are made up of several superposed shares. As the eigenvector function $b_k(t)$ always is a T-periodic function and consequently has the same period as the rotor revolution, the vibration of one degree of freedom can always be factorized into a Fourier series. The consequence is that the curves in the single degrees of freedom are a result of superposed sine and cosine functions with frequencies that are an integral multiple of the rotor cycle frequency. The frequencies for the single degrees of freedom which result from the Fourier analysis, are also shown in fig. 13a.

Fig. 13b shows all degrees of freedom oscillating with the same frequency which could be attributed to the fact that the introduced multiblade coordinates describe the system with constant coefficients even without analytical transformation. However, this is not

the case in the example given in fig. 13a. Thus, with a cyclic pitch angle unlike zero, the basic differential equation system with periodically-varying parameters can no longer be transformed using multiblade coordinates to a system with constant coefficients. This can be explained by the approaches introduced for the flap and lag motion:

$$\beta_k(t) = (a_{oo} + \Delta a_o) - (a_{1o} + \Delta a_1)\cos\psi_k - (b_{1o} + \Delta b_1)\sin\psi_k + \Delta b_o(-1)^{k-1} ,$$

$$\zeta_k(t) = (e_{oo} + \Delta e_o) + (e_{1o} + \Delta e_1)\cos\psi_k + (f_{1o} + \Delta f_1)\sin\psi_k + \Delta f_o(-1)^{k-1} , \qquad (9)$$

with a_{oo}, a_{10}, b_{10}, e_{oo}, e_{10}, and f_{10} as stationary values which can be determined in a trim calculation as a function of the collective and cyclic pitch angles. By adding the stationary values and the small irregularities, flap and lag angle can also be shortly described as

$$\beta(t) = \beta_o(t) + \Delta\beta(t) \quad , \qquad \zeta(t) = \zeta_o(t) + \Delta\zeta(t) . \qquad (10)$$

As β_o and ζ_o are functions of time (equation 9), the corresponding angular velocities and accelerations are as well determined:

$$\dot{\beta}_o = a_{1o}\,\Omega\sin\psi - b_{1o}\,\Omega\cos\psi \quad , \quad \dot{\zeta}_o = -e_{1o}\,\Omega\sin\psi + f_{1o}\,\Omega\cos\psi \quad ,$$

$$\ddot{\beta}_o = a_{1o}\,\Omega^2\cos\psi + b_{1o}\,\Omega^2\sin\psi \quad , \quad \ddot{\zeta}_o = -e_{1o}\,\Omega^2\cos\psi - f_{1o}\,\Omega^2\sin\psi \quad . \qquad (11)$$

In the equations of motion or system matrices respectively, products of the angles and their derivatives often occur, for instance in the balance of forces of the whole helicopter in x direction the term

$$\sum_{k=1}^{4} \dot{\zeta}_k^2\; b\,\sin\zeta_k\,\sin\psi_k\,m_b , \qquad (12)$$

which considers the centrifugal force of the four blades due to the lag motion. After inserting the perturbational approaches and linearizing, the result is

$$\sum_{k=1}^{4} b\,m_b \left[\dot{\zeta}_o^2\,\Delta\zeta + 2\dot{\zeta}_o\,\Delta\dot{\zeta}\,\zeta_o\right]_k \sin\psi_k \quad , \qquad (13)$$

where the constant terms and the products of the perturbation values have been neglected. By inserting the multiblade coordinates, terms result at last as for example

$$\sum_{k=1}^{4} b\,m_b \left\{\left[(e_{1o}\,\Omega\sin\psi)^2 + \ldots\right]\left[\Delta e_o + \Delta e_1\cos\psi_k + \Delta f_1\sin\psi_k + \Delta f_o(-1)^{k-1}\right] + \ldots\right\}\sin\psi_k \quad , \qquad (14)$$

which can be written as

$$b\,m_b\left[e_{1o}^2\,\Omega^2\sum_{k=1}^{4}\sin^4\psi_k\,\Delta f_1 + \ldots\right] . \qquad (15)$$

As this term can be found in one of the fuselage equations, the periodically-varying coefficients must consequently be eliminated only by inserting the multiblade coordinates. Here, however, the result is

$$b\,m_b\left[e_{1o}^2\,\Omega^2\left(\frac{1}{2}\cos 4\psi + \frac{3}{2}\right) + \ldots\right] . \qquad (16)$$

This way, the coefficient remains periodic!

In order to eliminate the periodically-varying coefficients in the blade equations analytically, they are multiplied besides other things with $\sin\psi_k$ or $\cos\psi_k$ and are summed up. This was described in detail by J. Dugundij and J.H. Wendell /2/. If trigonometric functions of the azimuth angle appear in third order in the basic form of the blade equations, periodically-varying coefficients continue to exist in these equations as well. When considering the difference form $b_o\,(-1)^{k-1}$ in the multiblade coordinate approach, the quantity

of the allowable rotor-harmonic frequencies in the system matrices is furtheron restricted; this concerns those frequencies or powers of the trigonometric functions respectively which do not impede the transformation into a system with constant coefficients. For a four-blade rotor, the multiblade coordinate approach presented here does only lead to a system with constant coefficients under the condition that the fuselage equations do not contain any powers of 4th order of the trigonometric functions and that the blade equations contain powers of first order exclusively. This way, the use of the pure multiblade coordinate approach with analytical transformation is extremely restricted. However, this is not the case for instance with a cyclic blade pitch ϑ_s, ϑ_c equal to zero; then e_{10}, f_{10}, a_{10}, $b_{10} = 0$ results from the trim calculation and, this way, $\dot{\beta}_0$, $\ddot{\beta}_0$, $\dot{\vartheta}_0$, $\ddot{\vartheta}_0 = 0$ as well and the terms with unfavourable powers of the trigonometric functions are dropped in the equations of motion, so that, consequently, the multiblade coordinates again describe the corresponding system with constant coefficients.

The eigenvalues, that means the modal dampings and eigenfrequencies, are only insignificantly changed at increasing cyclic pitch angles.

Systems with blade to blade dissimilarities

In order to investigate the influence of different blade characteristics, collective and cyclic pitch angles and, consequently, the stationary trim values were put to zero and individual blade dampings and stiffnesses were varied. It is easy to show analytically, that with different dynamic blade characteristics, the transformation to a system with constant coefficients can no longer be carried out with the help of the multiblade coordinate transformation. This becomes also evident in the graphic representation of the eigenvector functions: Among the individual components, different rotor harmonics come into being again. Moreover, the T-periodic vibration in a single component can again possess several parts with different multiples of the rotor cycle frequency. As an example, fig. 14 shows the coupling of collective and cyclic lag motion. The calculation was carried out for a deviation of the stiffness of a rotorblade at a rotor angular velocity of 10 rad/s. Due to the centrifugal force, the stiffness is extremely increased at growing rotational speed, with the relative dissimilarity $\Delta c_\vartheta / C_\vartheta$ in the stiffness becoming so small that the different frequencies or the superposition of different rotor harmonics in the components of the eigenvector functions respectively, cannot be recognized in the diagram. However, the superposition can be proved by the numerical calculation of the Fourier coefficients.

The blade to blade dissimilarities can also extremely influence the eigenvalues. Especially different damping characteristics, as for instance C.E. Hammond /6/ investigated in the case of an articulated rotor with one inoperative damper, can influence the stability. Fig. 15 shows the decrease of the modal damping of the lag regressing mode at increasing divergence in the damping of one or two rotor blades, respectively.

Air resonance

The mathematical model was also applied in a very simplified investigation of the air resonance in hover flight. To do this, landing gear dampers and landing gear stiffnesses were put to zero. Fig. 16 shows as a result the eigenvalues which had been converted for the system with constant coefficients. Of course, the results are not at all of any practical importance. They only serve to show the influence of the flap conus angle, which is stronger compared with that of the ground resonance investigation. The trim calculation was not carried out for the individual calculations, but the flap conus angle a_o was varied directly. It is shown that even at a flap conus angle of $a_o \approx 1{,}8^\circ$ the coupled roll-flap-lag motion becomes unsteady. At last, the coupled roll-pitch-fuselage motion becomes

unperiodic with decreasing flap conus angle. Two eigenvalues which also describe the flight mechanic behavior, characterize periods of T = 16,2 s and T = 13,9 s as well as the appertaining time in which the amplitude increases to its double value of T_D = 69 s and T_D = 40,6 s, this means they characterize an unsteady motion. These values result for $a_o = 3^o$. With decreasing a_o, one of the eigenvalues changes into the stable range. The flap conus angle has only little influence on the other eigenvalues. This significant change of the mentioned eigenvalues can be attributed to the Coriolis term from rotor rotation and flap motion in the balance of moments in the lag equation. A calculation without this term shows that the coupled roll-flap-lag motion is stable and that the coupled roll-pitch motion remains aperiodic at increasing flap conus angle.

For the rotor rotational speed of Ω = 45 rad/s, a trim calculation for the hover state resulted in a collective pitch angle $\vartheta_0 = 8,6^o$ and a flap conus angle of $a_o = 3,3^o$. Consequently, the chosen helicopter has an extreme instability. A variation of the rotor angular velocity with an adaption of collective blade pitch angle and flap conus angle in the trim calculation showed that this way the instability cannot be prevented. From literature, for instance D.P. Schrage, D.A. Peters /7/ and R.A. Ormiston /5/, it is well known that different kinds of coupling such as structural flap-lag coupling and pitch-lag coupling can significantly influence the stability of air resonance. In order to investigate these influences, the model is to be extended by the corresponding coupling terms. Moreover, the degrees of freedom in z direction (translation and yawing) are to be introduced, so that states in forward flight can be investigated as well. As has been shown by P.P. Friedmann, C. Venkatesan /8/ and J. Nagabushanam, G.H. Gaonkar /9/, a further significant complement is the introduction of the dynamic inflow which is important regarding the air and ground resonance investigations.

Conclusion

- In many cases, the combination of multiblade coordinates and Floquet theory produces results that are easy to interpret at acceptable numerical expenditure.
- The graphic representation of the eigenvector functions shows at once the practicability of a transformation into a system with constant coefficients using the multiblade coordinates and subsequent analytical transformations of the equations.
- Not only with blade to blade dissimilarities the multiblade coordinate transformation does not lead to a system with constant coefficients, but also by cyclic blade pitch angles, which can be attributed to unallowable frequencies in the system matrices due to the mathematical approach of multiblade coordinates with small perturbations.

Acknowledgement

The paper is based on research work funded by the Bundesministerium für Forschung und Technologie BMFT (Ministry of Research and Technology), contract LFF 84318.

References

/1/ Ewald, J. An Application of Floquet Theory to Investigate Helicopter Mechanical Instability Using a Spatial Model Including Rotor Blade Flapping, Eleventh European Rotorcraft Forum, 1983, Paper No. 63

/2/ Dugundji, J. Wendell, J.H. Some Analysis Methods for Rotating Systems with Periodic Coefficients, AIAA Journal, Vol. 21, No. 6, 1983

/3/ Hohenemser, K.H. Yin, S.K. Some Applications of the Method of Multiblade Coordinates, Journal of the American Helicopter Society, Vol. 17, No. 3, Juli 1972, pp. 3-12

/4/ King, S.P. Helicopter Ground Resonance, Experimental Validation of Theoretical Results by the Use of Scale Model, Eighth European Rotorcraft Forum, 1982, Paper No. 7.4

/5/ Ormiston, R.A. — Aeromechanical Stability of Soft Inplane Hingeless Rotor Helicopters, Third European Rotorcraft and Powered Lift Aircraft Forum, 1977, paper 25

/6/ Hammond, C.E. — An Application of Floquet Theory to Prediction of Mechanical Instability, Specialist Meeting on Rotorcraft Dynamics, AHS, 1974

/7/ Schrage, D.P. Peters, D.A. — Effect of Structural Coupling Parameters on the Flap-Lag Forced Response of a Rotorblade in Forward Flight Using Floquet Theory, Fourth European Rotorcraft and Powered Lift Aircraft Forum, 1978, paper No. 23

/8/ Friedmann, P.P. Venkatesan, C. — Influence of Various Unsteady Aerodynamic Models on the Aeromechanical Stability of a Helicopter in Ground Resonance, Second Decennial Specialists' Meeting on Rotorcraft Dynamics, Ames Research Center, Nov. 7-9, 1984

/9/ Nagabushanam, J. Gaonkar, G.H. — Rotorcraft Air Resonance in Forward Flight with Various Dynamic Inflow Models and Aeroelastic couplings, Ninth European Rotorcraft Forum, 1983, paper No. 52.

Appendix

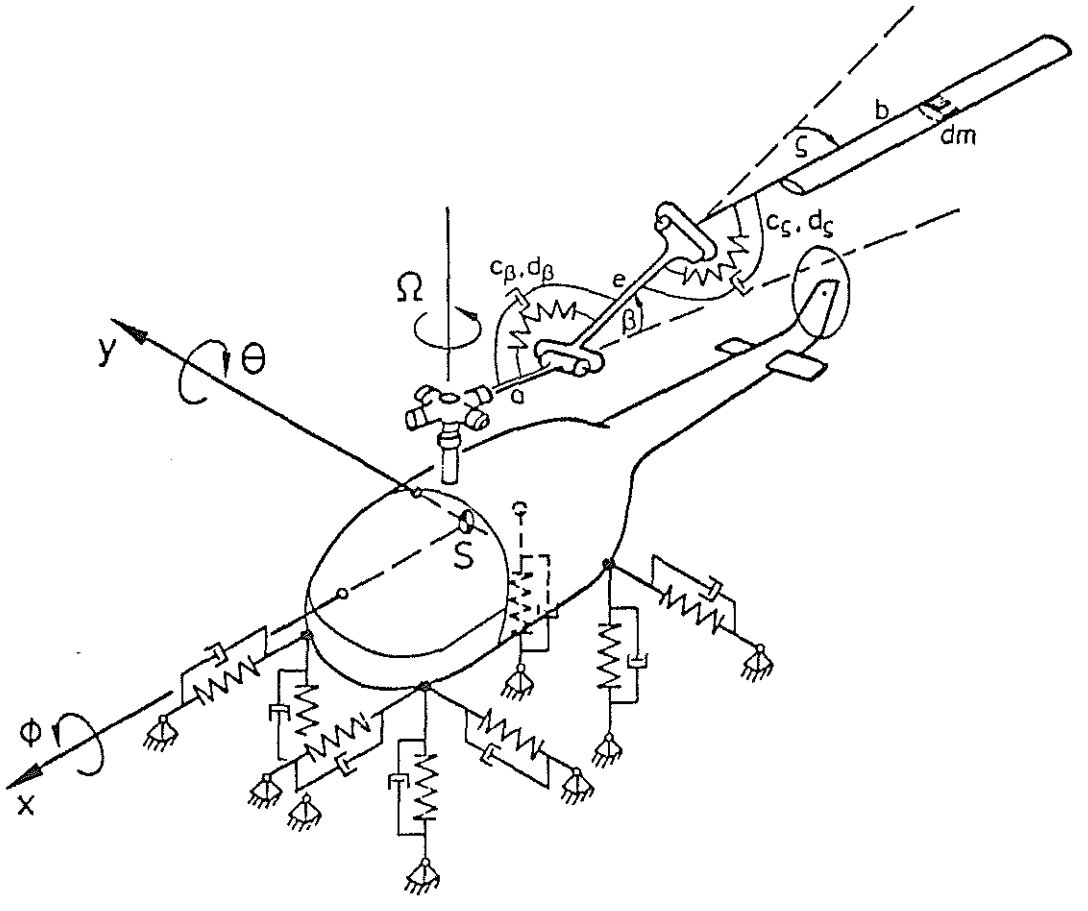

Fig. 1 Mathematical ground resonance model

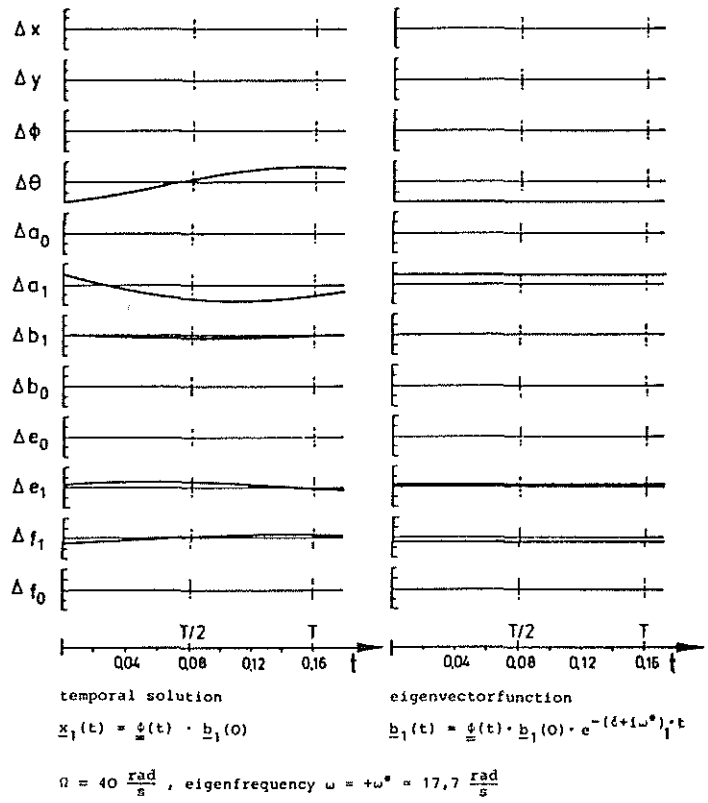

Fig. 2 Temporal solution and eigenvectorfunction of one eingenvalue (body pitch mode)

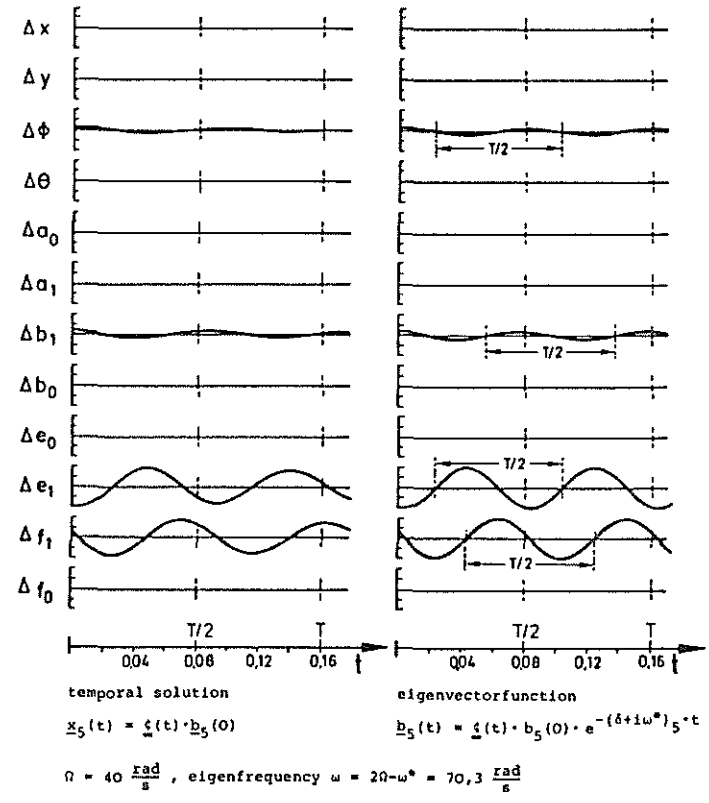

Fig. 3 Temporal solution and eigenvectorfunction of one eigenvalue (progressing lag mode)

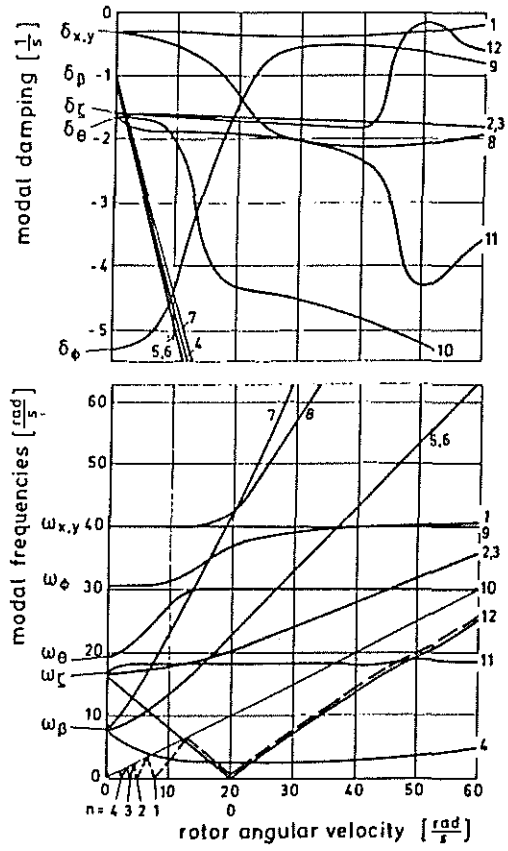

Fig. 4 Modal damping and eigenfrequencies of the corresponding system with constant parameters

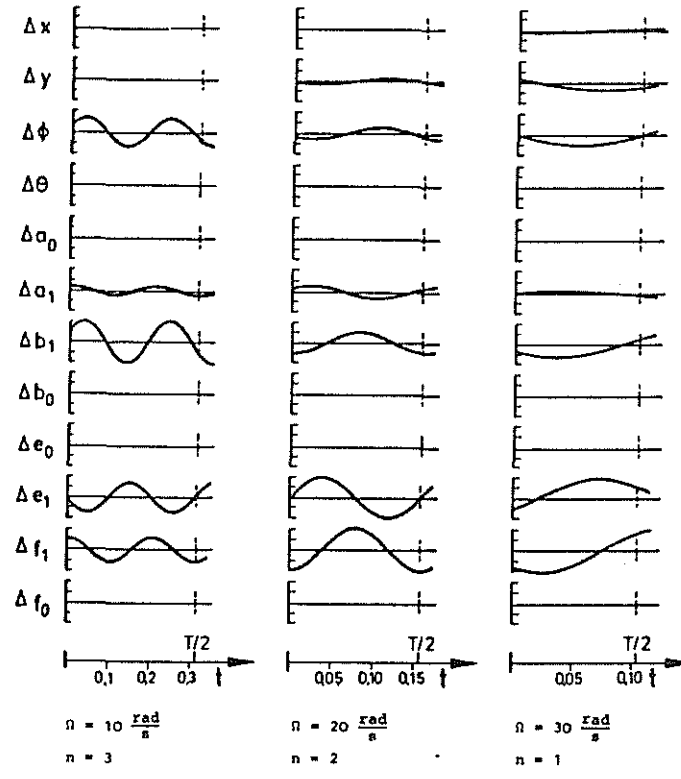

Fig. 5 Mode of vibration (eigenvectorfunction) for curve 9 at rotor angular velocity Ω = 10,20,30 rad/s

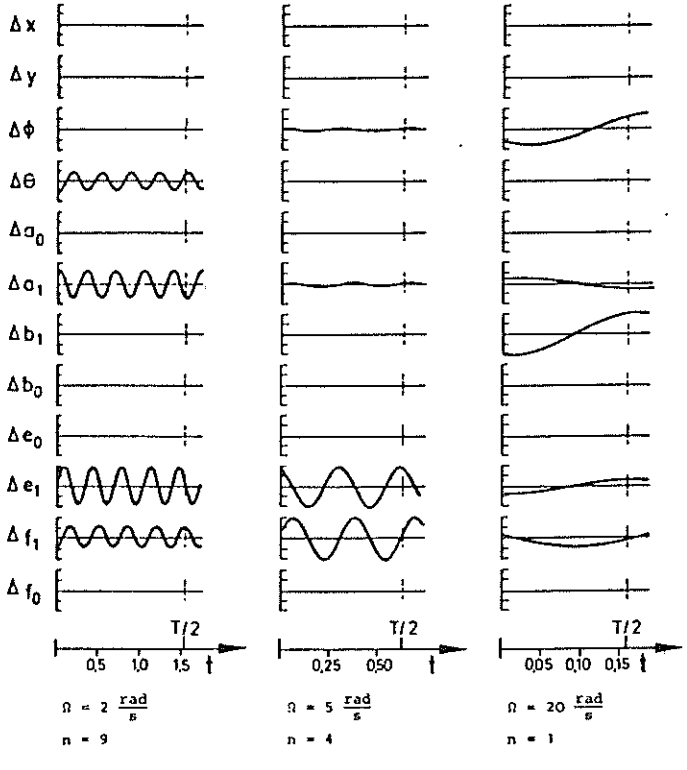

Fig. 6 Mode of vibration (eigenvectorfunction) for curve 10 at rotor angular velocity $\Omega = 2,5,20\ \frac{rad}{s}$

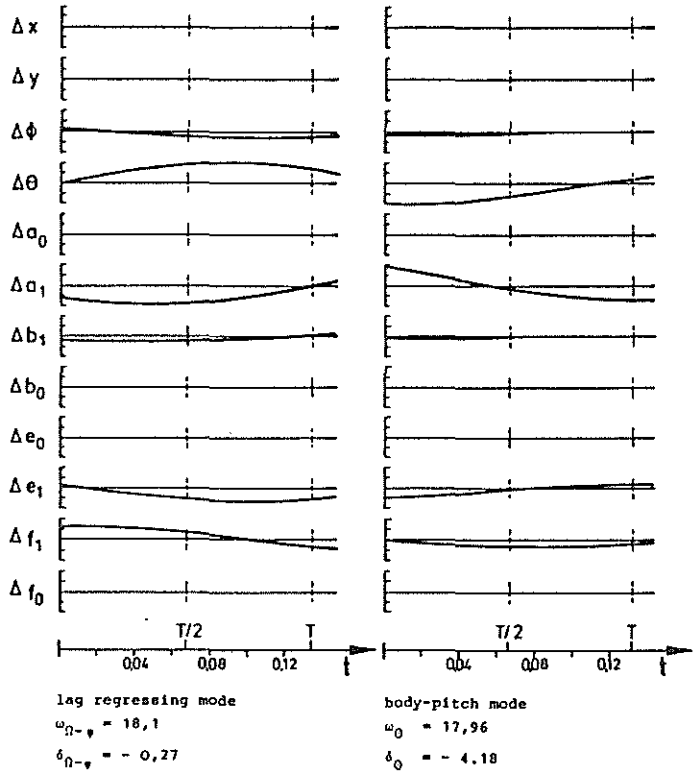

Fig. 7 Body pitch mode (curve 11) and lag regressing mode (curve 12) near 'resonance' frequency

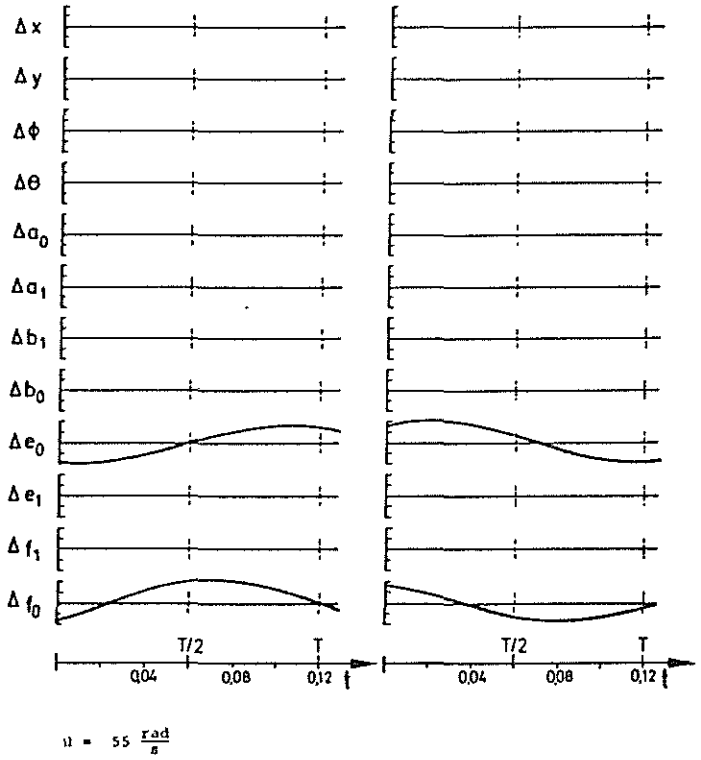

Fig. 8 Modes of vibration for double eigenvalues (collective lag mode)

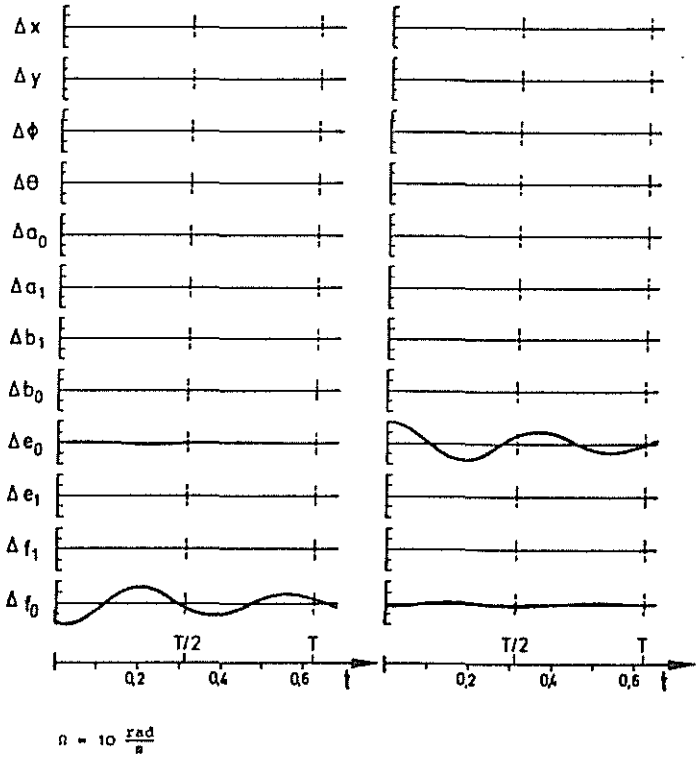

Fig. 9 Modes of vibration for double eigenvalues (collective lag mode)

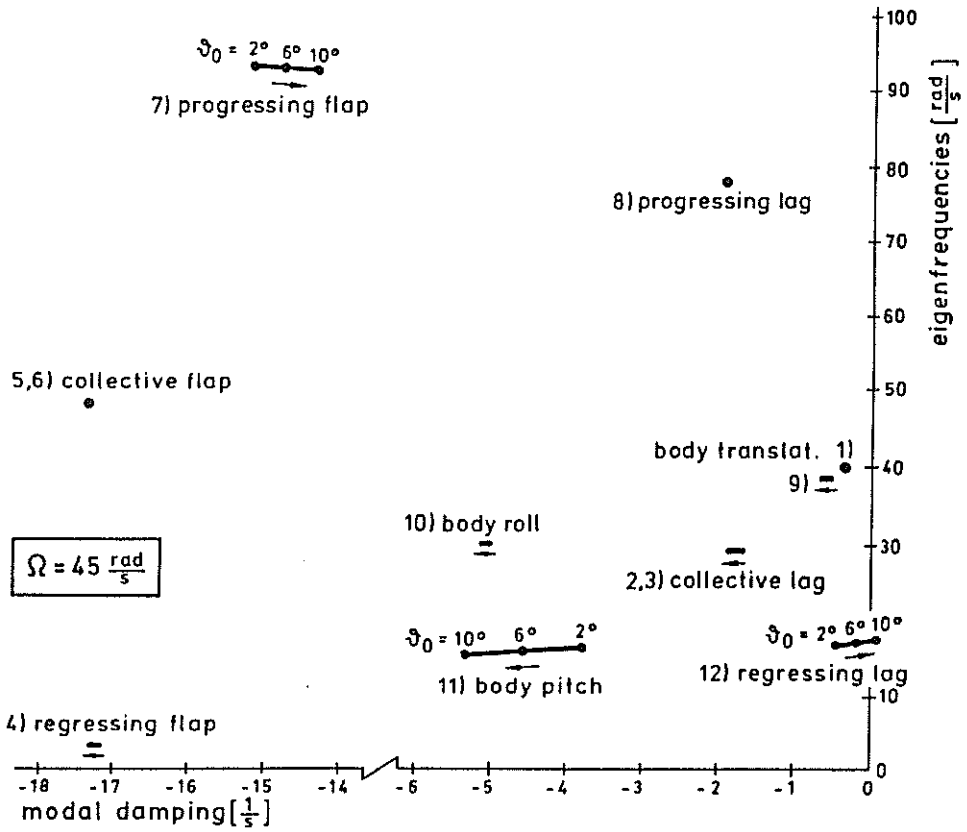

Fig.10 Variation of eigenvalues with increasing collective pitch

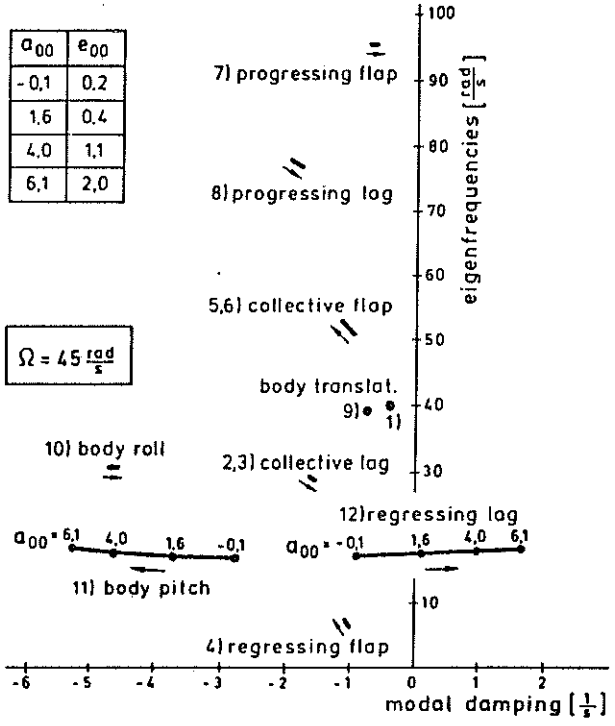

Fig.11 Variation of eigenvalues with increasing flap conus angle (collective pitch) without aerodynamic damping

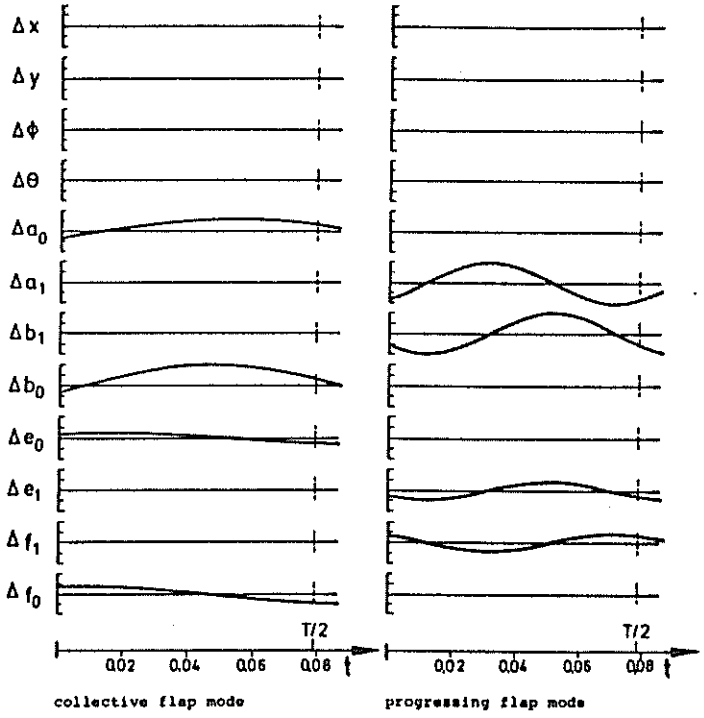

Fig.12 Collective and progressing flap mode at large flapping conus angle (a_o = 7°)

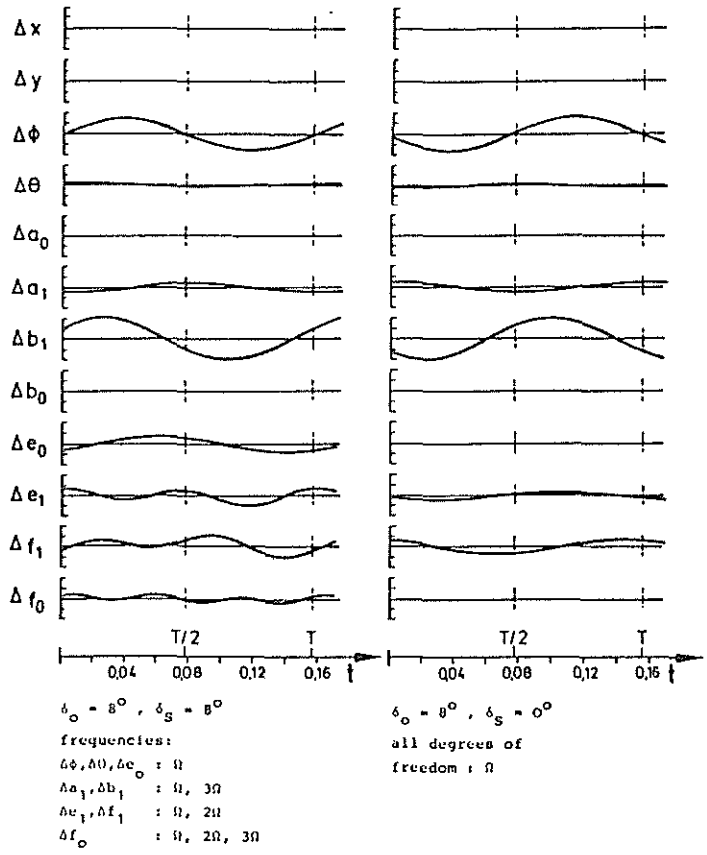

Fig.13 Body roll mode (eigenvectorfunction) at $\Omega = 40\ \frac{rad}{s}$ with cyclic pitch $\delta_S = 8^\circ$ and $\delta_S = 0^\circ$

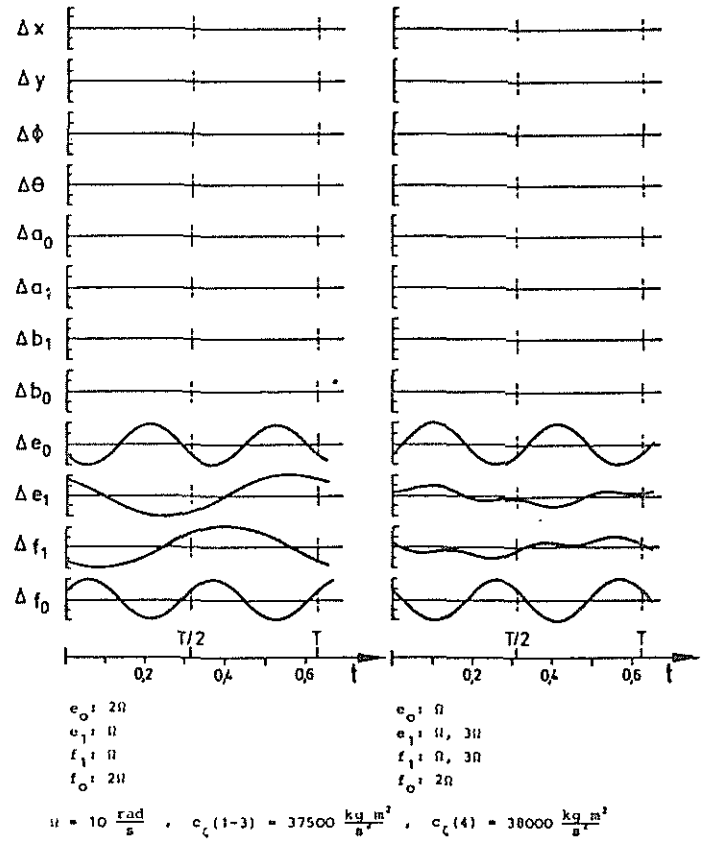

Fig.14 Coupling of collective and cyclic lag motion at different blade stiffness

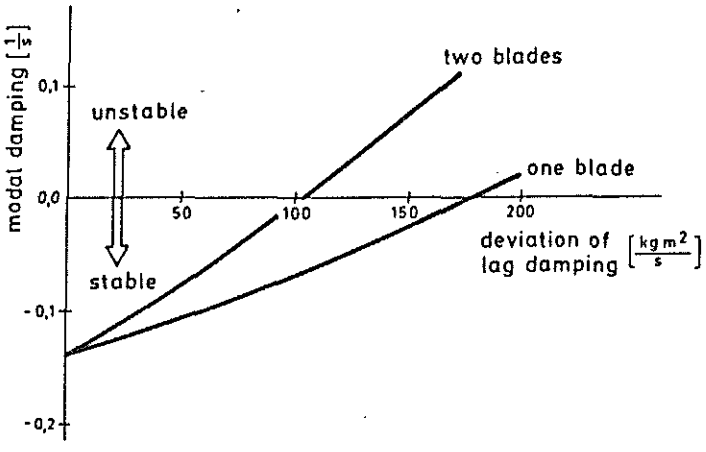

Fig.15 Modal damping of the lag regressing mode at different blade damping

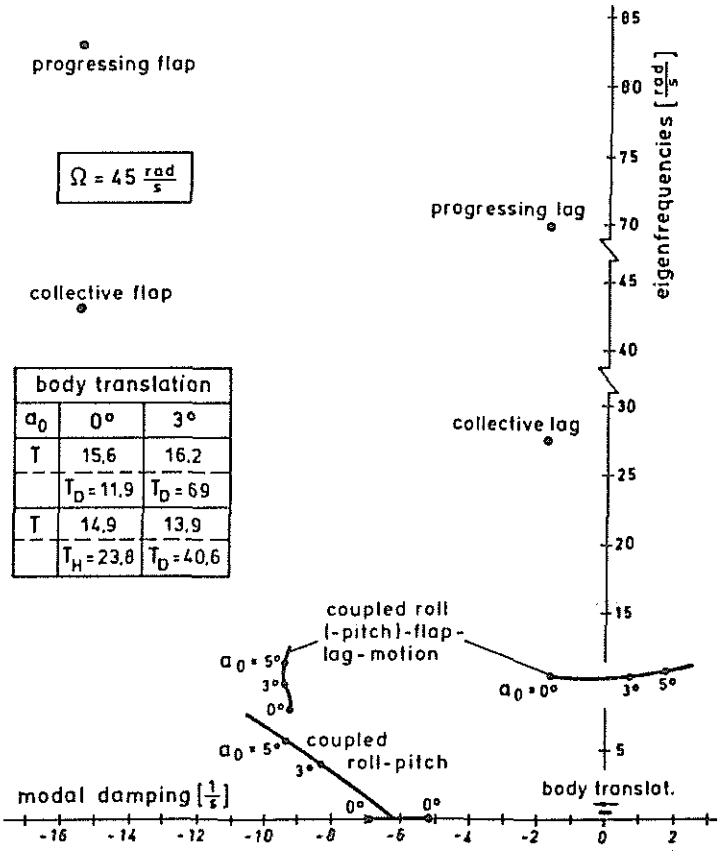

Fig.16 Variation of eigenvalues with increasing flapping conus angle (air resonance)